Simulation-guided preparation of 3D in vitro models with predictable oxygen distribution

Talia Hertzberg, Biomedical Engineering
Mentor: Vikram D. Kodibagkar, Associate Professor
School of Biological and Health Systems Engineering

Background

- Understanding cellular responses to hypoxia and its pathological role can lead to sustainable treatment options[1]
- Key role of hypoxia [depletion of oxygen] in the progression of various diseases: cancer, stroke, and traumatic injuries[2]
- Several *in vitro* studies have been carried out to understand the cellular response to hypoxia, however, most were under non-physiological hypoxic/normoxic conditions and/or 2D cultures[3]
- Oxygen delivery within the tissue (beyond blood vessels) occurs through the process of gas diffusion, which leads to oxygen concentration gradients[3]
- Importance of *in vitro* models recapitulating the physiological state (i.e. natural tissue), as cellular behavior can be greatly affected by the surrounding environment[4]
- Heterogeneity in the tissue can be caused by perfusion, oxygen consumption rate of cells, and composition of the tissue[5]
- The application of a magnetic resonance imaging (MRI)-based oximetry technique, "proton imaging of siloxanes, to map tissue oxygenation levels (PISTOL)", was developed in our lab[1,6-9] and has advantages over standard oximetry methods
- Non-invasively obtaining quantitative pO_2 maps of any desired slice within the tissue

## Methods & Materials

Simulation
- Simulations of the $O_2S3DMRS$ were performed by COMSOL Multiphysics using the Transport of Diluted Species module
- The anatomization of both simulation and experimental 3D models will coincide with each other, assessing tissue oxygenation at normoxic (0.2 mM) and hypoxic (0 mM) levels
- 3D cylindrical sponge infused with cells in the pores containing gel with an outside environment of polydimethylsiloxane (PDMS)
- Simulation slices will provide a predicted range of pO_2 values from the determined physics and limited input parameters
- Stationary studies assessed how fast cell consumption occurred through oxygen diffusion in the experimental $O_2S3DMRS$
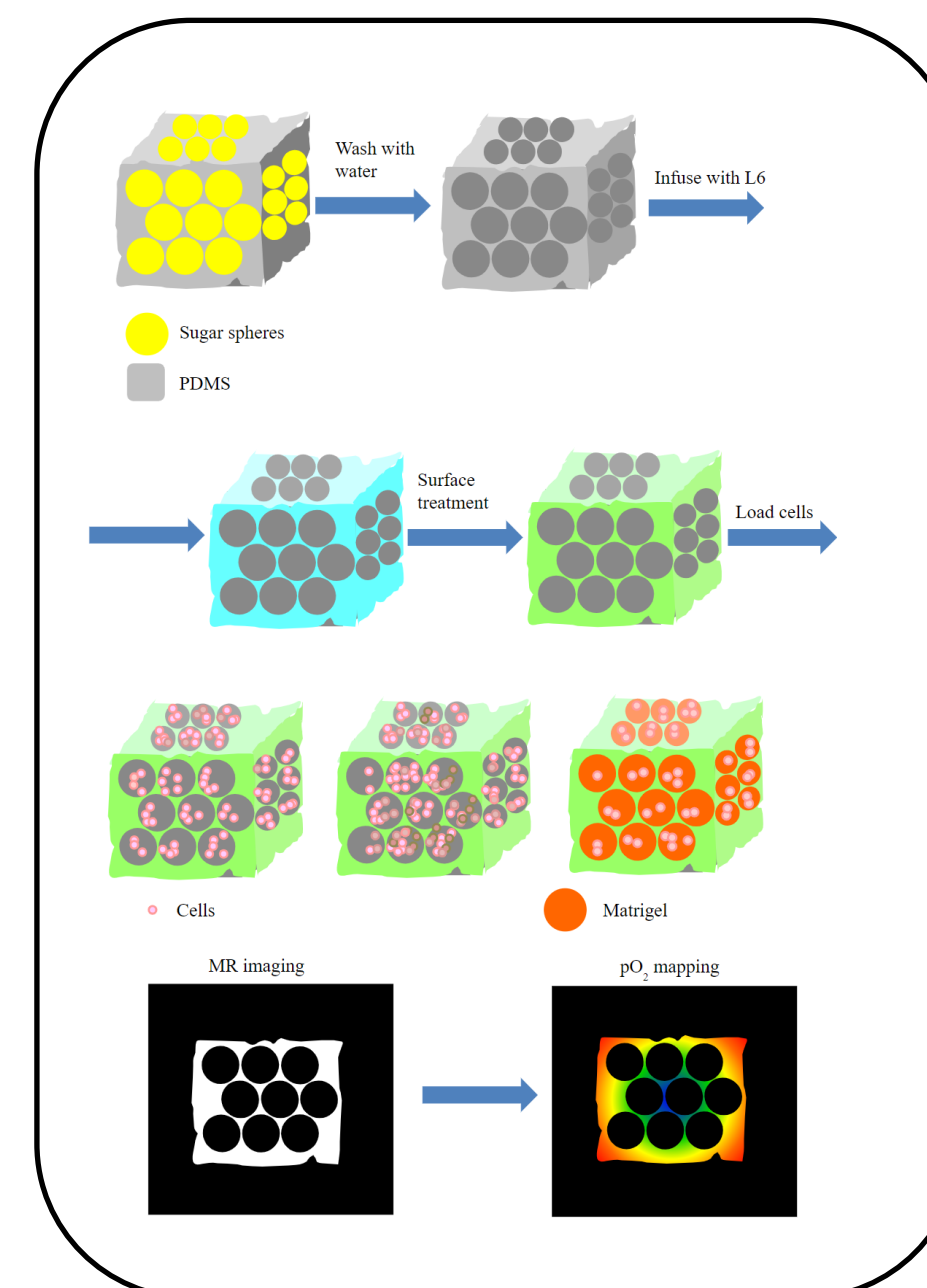
Experimental
- Preparation of scaffold will be done by establishing a hexagonal closed packed structure of sugar spheres (Suglets®) into a 3D cylindrical mold
- PDMS will be made through aliquoting Sylgard 184 base/crosslinker together around the sugar mold to then be vacuumed, cured, soaked in L6 (an MRI pO_2 reporter molecule Tetradecamethylhexasiloxane (L6)), washed in phosphate buffered saline, and applied a surface treatment to help create a more hydrophilic surface for cell seeding after cell culturing
- Cell (NIH 3T3 fibroblasts, H1975 lung cancer) viability/proliferation will be monitored using alamar blue assay
- In the future, the MRI oximetry technique of PISTOL will analyze images of the pO_2 present in the $O_2S3DMRS$

Motivation

- Assess tissue oxygenation in 3D *in vitro* models containing cell cultures by simulations and O_2 sensitive 3D-MR scaffolds ($O_2S3DMRS$)
- Provide a testbed for hypoxia-targeted MR imaging and therapeutic agents
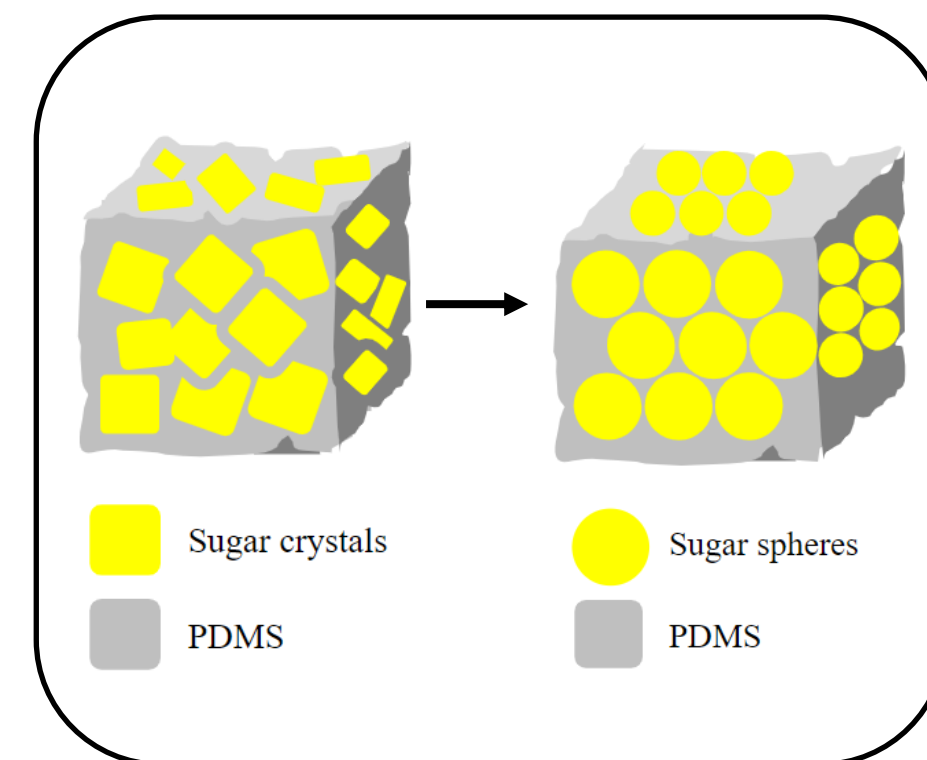

Fig. 1 Schematic: Original sugar crystal template **(left)** versus the new sugar sphere hexagonal closed-pack structure **(right)** of experimental $O_2S3DMRS$. The sugar crystals are representing a disordered packing arrangement while the spheres are ordered according to each layer.
Courtesy of Sugamura **(left)**

Fig. 2 Block Diagram: Newer schematic of experimental $O_2S3DMRS$ with cell seeding, leading to MR imaging.

Simulation Results
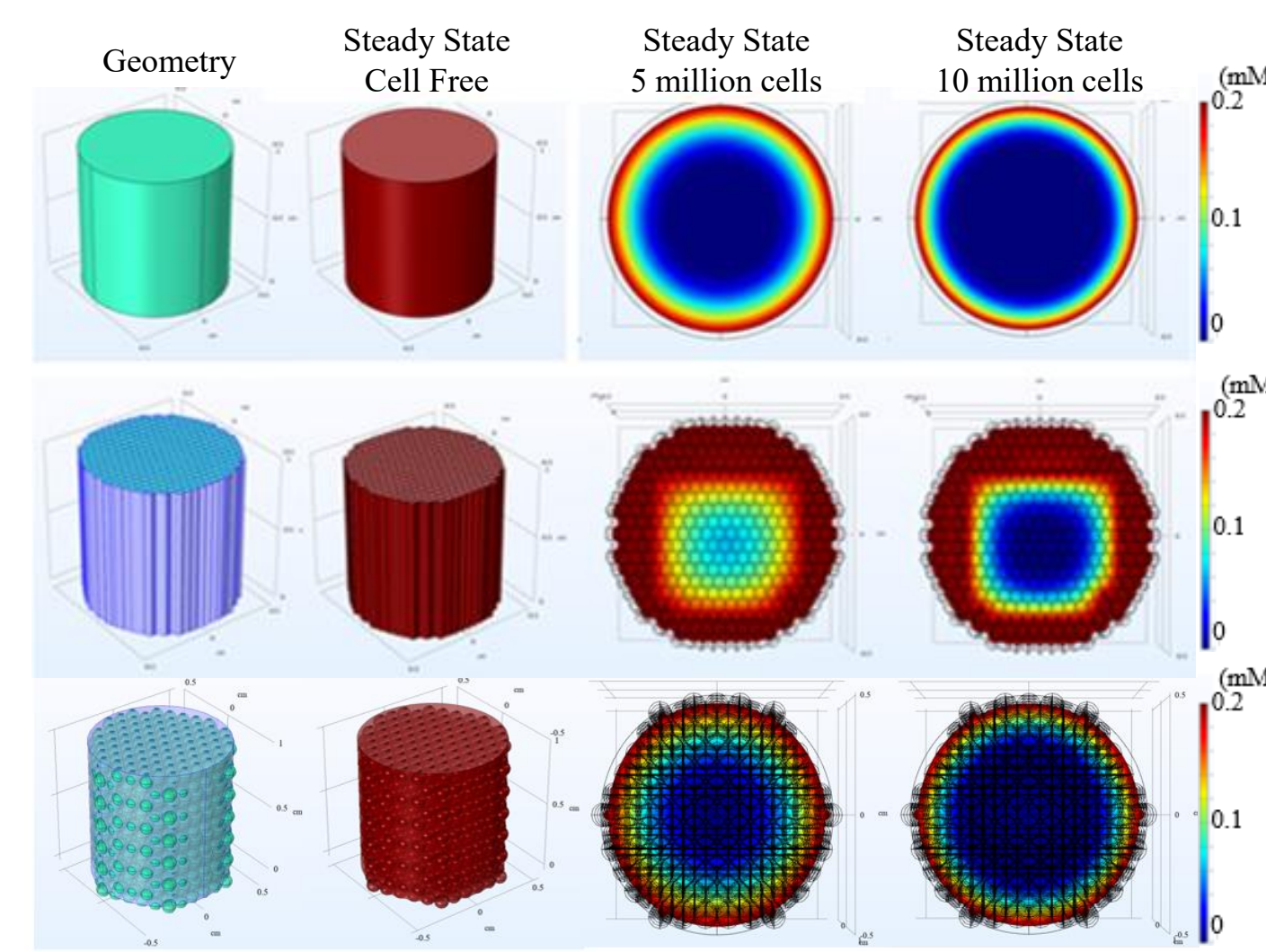
Fig. 3 Simulation of steady state oxygenation within hydrogel (top row), engineered cylindrical pore sponge (middle row), and $O_2S3DMRS$ (bottom row) under normoxic boundary. Color bars indicate the O_2 concentration where 0.2 mM O_2 corresponds to normoxic condition (21% pO_2).

$$Air = 21\% = 160\ torr = 0.2\ mM\ O_2$$
$$Hypoxia\ Threshold = 10\ torr = x\ mMO_2$$

$$\frac{0.2\ mM}{160\ torr} = \frac{x\ mM}{10\ torr}$$

$$x\ mM = \frac{0.2\ mM}{16} = 0.0125\ mM$$

Fig. 4 Sample calculation for hypoxia binding threshold
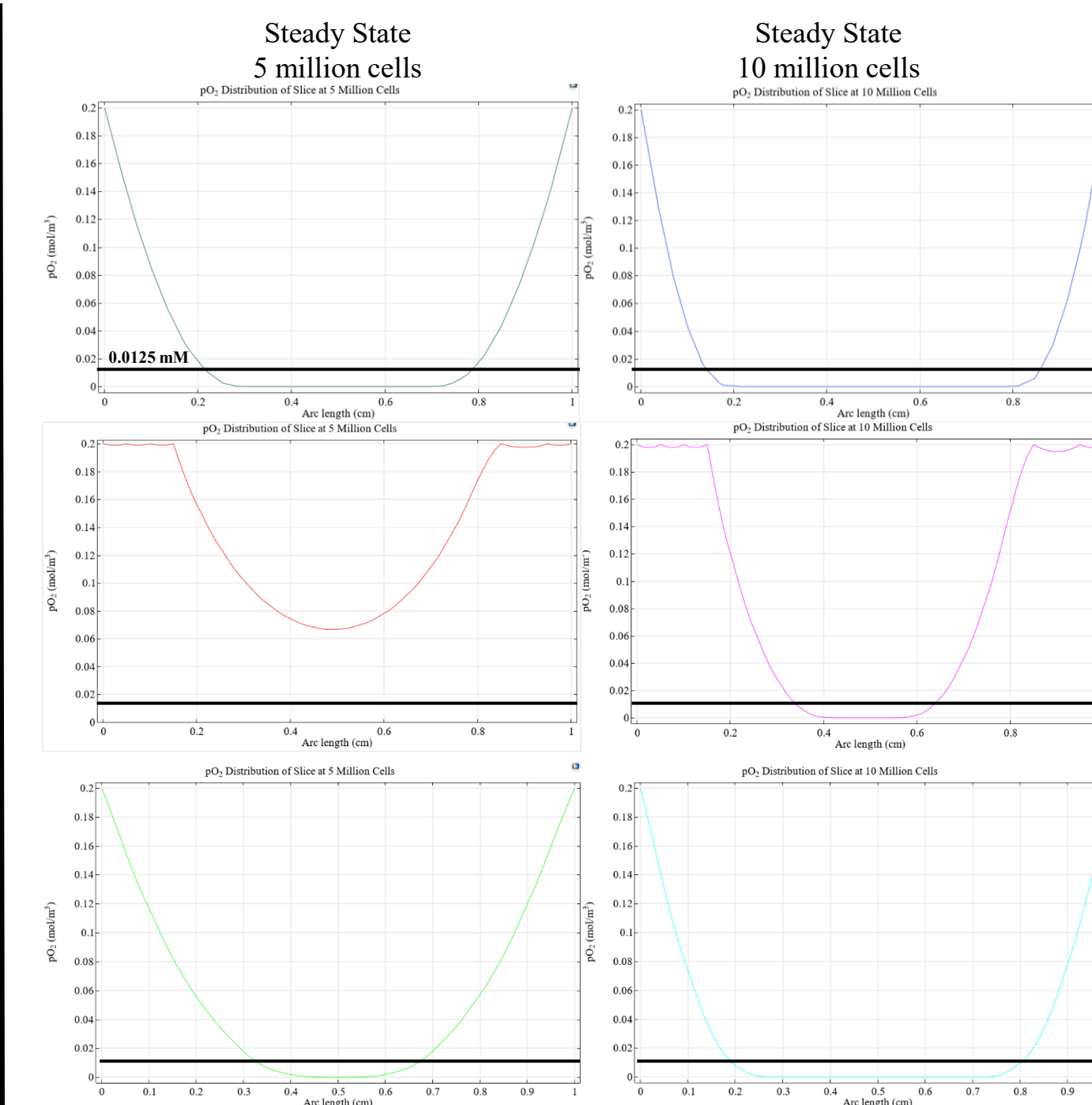
Fig. 5 Line graphs represent gel phantom (top row), engineered cylindrical sponge (middle row), and the $O_2S3DMRS$ (bottom row) from **Fig. 3** simulating the pO_2 distribution across steady state conditions for 5 and 10 million cells. Black horizontal line represents the threshold of where hypoxia targeting agents bind (0.0125 mM).

Experimental Results
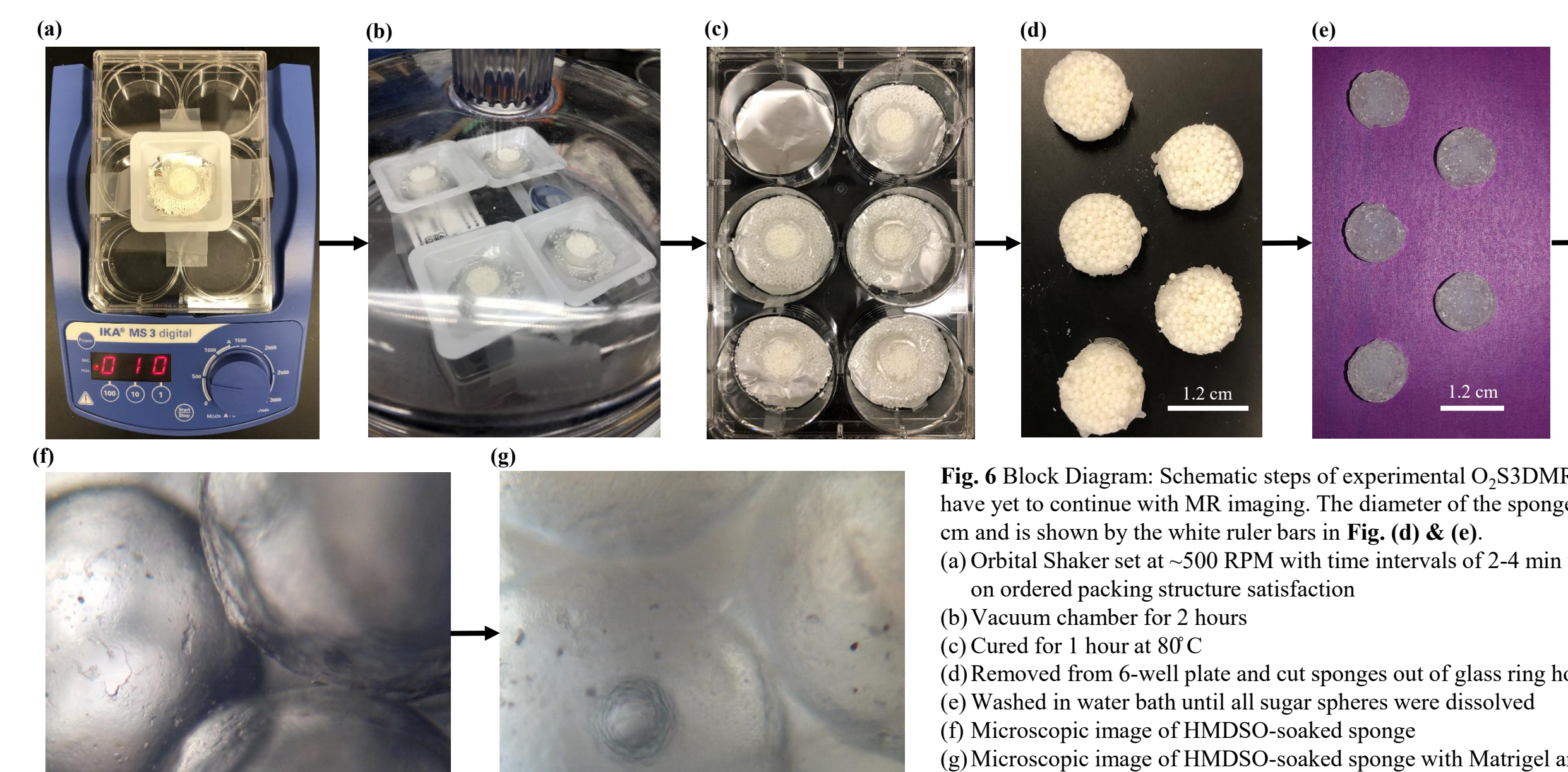
Fig. 6 Block Diagram: Schematic steps of experimental $O_2S3DMRS$ with cell seeding, have yet to continue with MR imaging. The diameter of the sponge is approximately 1.2 cm and is shown by the white ruler bars in **Fig. (d) & (e)**.
(a) Orbital Shaker set at ~500 RPM with time intervals of 2-4 min that were repeated based on ordered packing structure satisfaction
(b) Vacuum chamber for 2 hours
(c) Cured for 1 hour at 80°C
(d) Removed from 6-well plate and cut sponges out of glass ring holders
(e) Washed in water bath until all sugar spheres were dissolved
(f) Microscopic image of HMDSO-soaked sponge
(g) Microscopic image of HMDSO-soaked sponge with Matrigel and 5 million seeded cells

Results & Discussion

Results
- The current $O_2S3DMRS$ in **Fig. 3** contains cylindrical pores (middle row) and spherical pores (bottom row) representing the cells-laden hydrogel with an outer PDMS coating both having specified diffusion coefficients in relation to a gel phantom
- The O_2 concentration at 0.25 cm from the center was 0.10-0.12 mM for cylindrical pores and 0.02-0.04 mM for spherical pores in the $O_2S3DMRS$ compared to 0 mM for the gel phantom of the same dimension at steady state with 5 million cells
- At 10 million cells the O_2 concentration at the same location and dimension reported 0.06-0.08 mM and 0 mM, cylindrical and spherical, respectively, for the sponge versus the gel at 0 mM
- Increased O_2 penetration in the sponge
- It is concluded thus far that the porous scaffolds are better oxygenated as compared to the gel model
- Line graphs represent the oxygenation across a cut line through the slices depicted in **Fig. 3**
- Changes in pO_2 occur from diffusion of the outer edges to the center of the slice
- The black horizontal line on the graph is the threshold at which hypoxia targeting agents start to bind. The calculation is derived in **Fig. 4**, in which the threshold lies around 10 torr or 0.0125 mM

Discussion
- Seed cells within the pores of the sponges and assess the pO_2 of their surrounding environment
- Survival rate of cells based on the level of oxygenation
- Only simulation and experimental results have been recorded with future analysis of MR imaging to obtain pO_2 maps to locate the oxygenation in the $O_2S3DMRS$
- Current MR contrast agent being used, hexamethyldisiloxane (HMDSO), a small linear liquid siloxane, can detect pO_2 through MR imaging
- pO_2 distribution of this MR pO_2 reporter molecule
- Predicted values of pO_2 distribution obtained from the simulation will be differentiated from the empirical values recorded from the pO_2 PISTOL maps to determine the reliability of MR hypoxia-targeted *in vitro* testing

Future Work
- MR experimentation through PISTOL[1]
- Evaluating different hypoxia contrast agents[1]
  - Validation of imaging agents
    - After comparing both experimental and simulation scaffold results

Acknowledgements
I would like to acknowledge the ProBE Research Lab under the direction of Dr. Vikram Kodibagkar and for the assistance of graduate mentor Yuka Sugamura. Thank you both for your incredible mentorship and support.

References
[1] Agarwal S, et al. *Scientific Reports.*10(1):1399.
[2] Fabian Z. In: Ray S, ed. *Thermodynamics and Molecular Control*: IntechOpen; 2018.
[3] Pavlacky J, Polak J. *Front Endocrinol (Lausanne).* 11:57-57.
[4] Justice BA, et al. *Drug discovery today.*14(1-2):102-107.
[5] McMurtrey RJ. *Tissue Engineering Part C: Methods.* 22(3):221-249.
[6] Kodibagkar VD, et al. *Magnetic resonance in medicine.*55(4):743-748.
[7] Gulaka PK, et al. *NMR in biomedicine.*24(10):1226-1234.
[8] Menon JU, et al. *Theranostics.*2(12):1199-1207.
[9] Addington CP, et al. *Annals of biomedical engineering.* 44(3):816-827.
[10] Weaver JD, et al. *Biomaterials.*172:54-65.